Theoretical Insights Into the Hydrated (10.4) Calcite Surface: Structure, Energetics, and Bonding Relationships

ARTICLE *in* LANGMUIR · APRIL 2009

Impact Factor: 4.46 · DOI: 10.1021/la803652x · Source: PubMed

3 AUTHORS:

Adrián Villegas-Jiménez
Carnegie Institution for Science
7 PUBLICATIONS **71** CITATIONS
SEE PROFILE

Alfonso Mucci
McGill University
193 PUBLICATIONS **7,706** CITATIONS
SEE PROFILE

Michael Whitehead
McGill University
223 PUBLICATIONS **2,478** CITATIONS
SEE PROFILE

Langmuir
Article
pubs.acs.org/Langmuir

Theoretical Insights into the Hydrated (10.4) Calcite Surface: Structure, Energetics, and Bonding Relationships

Adrián Villegas-Jiménez,*,† Alfonso Mucci,† and Michael A. Whitehead‡

†*Earth and Planetary Sciences, McGill University and GEOTOP-McGill-UQAM, 3450 University Street, Montréal, Québec H3A 2A7, Canada, and* ‡*Chemistry, McGill University, 801 Sherbrooke Street West, Montréal, Québec, Canada*

Received November 3, 2008. Revised Manuscript Received February 7, 2009

Roothaan−Hartree−Fock molecular orbital methods were applied to investigate the ground-state structural, energetic properties, and bonding relationships of the hydrated (10.4) calcite surface. The adsorption of water molecules was modeled at the 6-31G(d,p) level of theory using $Ca_n(CO_3)_n$ slab cluster models ($4 \le n \le 18$) with a varying number of H_2O monomers ($2 \le (H_2O)_n \le 6$) interacting with the surface. Modeling results add fresh insights into the detailed 3D structural registry of the first and second hydration layers and the reconstructed (10.4) calcite surface, complementary to the information acquired from earlier atomistic, density functional, X-ray scattering, and grazing incidence X-ray diffraction studies. Both the modeled energies and geometries agree best with results of earlier density functional calculations, supporting the associative character of adsorbed water molecules. Two adsorption configurations are postulated: (i) H_2O molecules interacting with surface Ca through ionic bonding and by hydrogen bonding to a surface O with their dipole slightly oblique above the surface (1st hydration layer), and (ii) H_2O molecules that hydrogen bond to surface O and to H_2O molecules in the first hydration layer with their dipole nearly parallel to the surface (2nd hydration layer). These interactions are consistent with the "chemisorption" and "physisorption" of H_2O on calcite surfaces, proposed on the basis of previous thermogravimetric and Fourier-transformed infrared studies. Most significant is the distortion of the surface Ca−O octahedra caused by the relaxation (and possibly rupture) of some Ca−O bonds upon hydration, weakening the topmost atomic layer. These findings are consistent with interpretations of X-ray photoelectron spectroscopy, density functional theory, and electrokinetic studies that suggest the preferential release of surface Ca atoms over surface CO_3 groups upon hydration of the cleavage surface. These insights will help to elucidate mechanisms of carbonate mineral dissolution, the rearrangement of surface layers, ion replacement, charge development, and solute transport through subsurface lattice layers.

Introduction

Among $CaCO_3$ polymorphs, calcite is the most abundant and ubiquitous form in natural aquatic environments, where it plays a critical role on the regulation of pH, alkalinity, and heavy metal transport/mobility through exchange and coprecipitation reactions.[1] Calcite finds numerous industrial applications that range from the production of paper, paints, plastics, pharmaceuticals, and cosmetics to raw material in the construction industry and agriculture.[2,3]

Given its environmental significance and broad industrial applications, calcite has been the subject of extensive experimental studies,[4−7] which revealed the critical role that its surface properties play on the macroscopic chemical behavior of this mineral in aqueous suspensions. These properties result from the interplay of intermolecular and surface forces, such as hydrogen bonding, van der Waals interactions, and solvation at the mineral surface water interface.[8,9] Hydration is the most fundamental phenomenon to which dry mineral surfaces are subjected when immersed in aqueous solution. Surface forces modify the structure and properties of adsorbed and interfacial water, relative to the bulk solution, by breaking down water clusters and limiting the ability of H_2O molecules to reorient their dipoles,[9] which affects the properties of the mineral surface.

Surface-sensitive, noninvasive, X-ray, electron diffraction, and spectroscopic techniques as well as atomic force microscopic methods were used to investigate the structural properties of the calcite mineral−water interface.[10−19] They provided direct

*Corresponding author. Phone: (514) 398-4455 (ext. 00018). Fax: (514) 398-4680. E-mail: adriano@eps.mcgill.ca.

(1) Morse, J. W.; Mackenzie, F. T. *Geochemistry of Sedimentary Carbonates*; Dev. Sedimentol. 48; Elsevier: Amsterdam, 1990; Chapter 1.
(2) Vanerek, A.; Alince, B.; Van de Ven, T. G. M. *J. Pulp Paper Sci.* **2000**, *26*(9), 317–322.
(3) Usher, C. R.; Michel, A. E.; Grassian, V. H. *Chem. Rev.* **2003**, *103* 4883–4939.
(4) Morimoto, T.; Kishi, J.; Okada, O.; Kadota, T. *Bull. Chem. Soc. Jpn.* **1980**, *53*(7), 1918–1921.
(5) Ahsan, T. *Colloids Surf.* **1992**, *64*, 167–166.
(6) Davis, J. A.; Fuller, C. C.; Cook, A. D. *Geochim. Cosmochim. Acta* **1987**, *51*, 1477–1490.
(7) Zachara, J. M.; Cowan, C. E.; Resch, C. T. *Geochim. Cosmochim. Acta* **1991**, *55*, 1549–1562.
(8) Sposito, G. In *Mineral-Water Interface Geochemistry*; Hochella, M. F., Jr., White, A. F., Eds.; Mineralogical Society of America, Rev. Mineral. Geochem.: Washington, DC, 1990; Vol. 23, p 261.
(9) Israelachvili, J. *Intermolecular and Surface Forces*, 2nd ed.; Academic Press: San Diego CA, 1992; p 450.
(10) Stipp, S. L. S.; Hochella, M. F.Jr. *Geochim. Cosmochim. Acta* **1991**, *55*, 1723–1736.
(11) Chiarello, R. P.; Wogelius, R. A.; Sturchio, N. *Geochim. Cosmochim. Acta* **1993**, *57*(16), 4103–4110.
(12) Stipp, S. L. S.; Eggleston, C. M.; Nielsen, B. S. *Geochim. Cosmochim. Acta* **1994**, *58*(14), 3023–3033.
(13) Liang, Y.; Lea, A. S.; Baer, D. R.; Engelhard, M. H. *Surf. Sci.* **1996**, *351*, 172–182.
(14) Stipp, S. L. S. *Geochim. Cosmochim. Acta* **1999**, *63*(19/20), 3121–3131.
(15) Pokrovsky, O. S.; Mielczarski, J. A.; Barres, O.; Schott, J. *Langmuir* **2000**, *16*, 2677–2688.
(16) Neagle, W.; Rochester, C. H. *J. Chem. Soc., Faraday Trans.* **1990**, *86*(1), 181–183.
(17) Fenter, P.; Geissbühler, P.; DiMasi, E.; Srajer, G.; Sorensen, B. Sturchio, N. C. *Geochim. Cosmochim. Acta* **2000**, *64*(7), 1221–1228.
(18) Geissbühler, P.; Fenter, P.; DiMasi, E.; Srajer, G.; Sorensen, L. B.; Sturchio, N. C. *Surf. Sci.* **2004**, *573*, 191–203.
(19) Magdans, U.; Gies, H.; Torrelles, X.; Rius, J. *Eur. J. Mineral.* **2006**, *18* 83–92.

characterization of the molecular structure of the hydrated calcite surface, revealing a degree of surface reconstruction upon hydration. In addition, recent X-ray scattering[18] and grazing incidence X-ray diffraction[19] studies unveiled, for the first time, 3D structural details (interlayer spacing, interatomic distances, and lateral registry) of the hydrated (10.4) calcite surface.

Similarly, molecular modeling techniques are powerful tools to investigate the energy and structure of hydrated $CaCO_3$ surfaces. Several computer-assisted atomistic simulations (force-field-based) of the H_2O interactions with calcite and magnesium-bearing calcite surfaces were performed by numerous research groups.[20−33] Despite small discrepancies in the estimated interatomic distances between surface atoms and H_2O molecules, results of most studies suggested the formation of a monolayer of associatively adsorbed H_2O in a nearly flat arrangement, relative to the surface, adopting a herringbone pattern.[20,21,28,29] A slight vertical displacement of surface Ca atoms and rotation of the surface CO_3 groups were also reported in these studies.

Electronic structure studies, based on density functional theory (DFT), investigated the hydration of the (10.4) calcite surface[28,29,34,35] and examined its surface composition upon contact with a gaseous phase containing H_2O and $CO_{2(g)}$.[34] Whereas some of these calculations[28,29] predict a similar configuration of the associatively adsorbed H_2O molecules to those of the atomistic studies,[20,21,29] the latter consistently overestimated the energies of dry and wet calcite surfaces because they do not contain explicit chemical information and lack the full electronic relaxation offered by DFT techniques.[28]

Ab initio molecular orbital methods have also been used to investigate the ground-state properties of $CaCO_3$ polymers and clusters. Roothaan−Hartree−Fock (RHF) techniques were applied to (i) investigate the bonding and charge distribution in $CaCO_3$ monomers,[36] (ii) study protonation and H_2O attachment to $CaCO_3$ monomers and dimers,[37] and (iii) evaluate the performance of different protocols to stabilize $Ca_n(CO_3)_n$ clusters of different size ($4 \leq n \leq 22$) expressing the (001) surface.[38] It was concluded that H_2O surrounding the calcite clusters, simulating hydration, stabilize the clusters while decreasing the time required to achieve the self-consistent-field (SCF) convergence. Finally, partial geometric optimizations of $Ca_n(CO_3)_n$ clusters ($n \leq 21$), where only the geometries of the adsorbates were optimized, were carried out to investigate the interactions of anionic collectors, oleate and oleoyl sarcosine anions, with the calcite surface with RHF/3-21G.[39] This study confirmed that moderately large $Ca_n(CO_3)_n$ cluster models ($n \geq 14$) are adequate surrogate models to correctly describe the effect of neighboring surface atoms, model the infinite calcite surface, and investigate adsorption reactions.

Despite all these efforts, no systematic ab initio molecular orbital study of the structure and energy of the hydration layers at the (10.4) calcite surface has been conducted. The present investigation is an extension of earlier studies, based on the application of RHF techniques to exploit the power of Roothan−Hartree−Fock methods using moderately large cluster models ($n = 18$), to properly represent the idealized stoichiometric (10.4) calcite surface and accurately describe hydrogen bonding.[40] The results from earlier atomistic simulations and DFT calculations were used to select reasonable geometric constraints on the clusters and assign an initial configuration to the H_2O molecules. A series of RHF/6-31G(d,p) partial geometric optimizations, involving specific "reactive" atoms at the (10.4) calcite surface and a varying number of H_2O molecules, were performed to obtain information on the structure, the energy, and the bonding relationships governing the hydration process.

Methods

Computational Methods and Cluster Models. *Gaussian 03* software[41] was used to perform the geometric optimizations of finite charge-neutral slabs (clusters) taken from the bulk calcite structure.[42] The ideal stoichiometric (10.4) cleavage plane was represented in the slab and adopted as the molecular model of the calcite surface as in earlier studies.[20,27−30,39] The validity of this representation was confirmed using a standard protocol devised to determine the most stable surface atomic configuration of oxide minerals according to residual charge and bond strength minimization criteria.[43]

Cluster models have been commonly used to study the electronic structure of carbonate[36−39] and metal oxide minerals.[44,45] Specifically, cluster models were found suitable for investigations of adsorption reactions on $CaCO_3$ surfaces.[36−39] Therefore, this approach was adopted throughout this study. The absence of periodic boundary conditions in cluster models requires a formalism to treat crystal structure terminations and prevent "edge effects". Hydrogen atoms are commonly used as terminators of covalent compounds[44] and oxide minerals,[40,44,45] but this approach is not suitable for systems in which hydrogen bonding is involved, as for H_2O adsorption.[40] In addition, for

(20) de Leeuw, N. H.; Parker, S. C. *J. Chem. Soc., Faraday Trans.* **1997**, *93*(3), 467–475.
(21) de Leeuw, N. H.; Parker, S. C. *J. Phys. Chem. B* **1998**, *102*, 2914–2922.
(22) de Leeuw, N. H.; Parker, S. C.; Hanumantha Rao, K. *Langmuir* **1998**, *14*, 5900–5906.
(23) de Leeuw, N. H.; Parker, S. C. *J. Chem. Phys.* **2000**, *112*(9), 4326.
(24) de Leeuw, N. H.; Parker, S. C. *Am. Mineral.* **2002**, *87*, 679–689.
(25) Kuriyavar, S. I.; Vetrivel, R.; Hegde, S. G.; Ramaswamy, A. V. Chakrabarty, D.; Mahapatra, S. *J. Mater. Chem.* **2000**, *10*, 1835–1840.
(26) Hwang, S.; Blanco, M.; Goddard, W. A.III *J. Phys. Chem. B* **2001**, *105*, 10746–10752.
(27) Wright, K.; Cygan, R. T.; Slater, B. *Phys. Chem. Chem. Phys.* **2001**, *3* 839–844.
(28) Parker, S. C.; Kerisit, S.; Marmier, A.; Grigoleit, S.; Watson, G. W. *Faraday Discuss.* **2003**, *124*, 155–170.
(29) Kerisit, S.; Parker, S. C.; Harding, J. H. *J. Phys. Chem. B* **2003**, *107* 7676–7682.
(30) Kerisit, S.; Parker, S. C. *J. Am. Chem. Soc.* **2004**, *126*, 10152–10161.
(31) Kerisit, S.; Cooke, D. J.; Spagnoli, D.; Parker, S. C. *J. Mater. Chem.* **2005**, *15*, 1454–1462.
(32) Stöckelmann, E.; Hentschke, R. *Langmuir* **1999**, *15*, 5141–5149.
(33) Perry, T. D. IV; Cygan, R. T.; Mitchell, R. *Geochim. Cosmochim. Acta* **2007**, *24*, 5876–5887.
(34) Kerisit, S.; Marmier, A.; Parker, S. C. *J. Phys. Chem. B* **2005**, *109*(39), 18211–18213.
(35) Archer, T. D. Ph. D. Thesis, University of Cambridge, 2004.
(36) Thackeray, D.; Siders, P. D. *J. Chem. Soc., Faraday Trans.* **1998**, *94* 2653–2661.
(37) Mao, Y.; Siders, P. D. *J. Mol. Struct. (Theochem)* **1997**, *419*, 173–184.
(38) Ruuska, H.; Hirva, P.; Pakkanen, T. A. *J. Phys. Chem. B* **1999**, *103*(32), 6734–6740.
(39) Hirva, P.; Tikka, H.-K. *Langmuir* **2002**, *8*, 5002–5006.
(40) Tossel, J. A.; Vaughan, D. J. *Theoretical Geochemistry: Applications of Quantum Mechanics in the Earth and Mineral Sciences*; Oxford University Press: New York, 1992; Chapters 3 and 5.
(41) Frisch, M. J. ; Trucks, G. W.; Schlegel, H. B.; Scuseria, G. E.; Robb, M. A.; Cheeseman, J. R.; Zakrzewski, V. G.; Montgomery, J. A.; Stratmann, R. E.; Burant, J. C.; Dapprich, S.; Millam, J. M.; Daniels, A. D.; Kudin, K. N.; Strain, M. C.; Farkas, O.; Tomasi, J.; Barone, V.; Cossi, M.; Cammi, R.; Mennucci, B.; Pomelli, C.; Adamo, C.; Clifford, S.; Ochterski, J.; Petersson, G. A.; Ayala, P. Y.; Cui, Q.; Morokuma, K.; Malick, D. K.; Rabuck, A. D.; Raghavachari, K.; Foresman, J. B.; Cioslowski, J.; Ortiz, J. V.; Baboul, A. G.; Stefanov, B. B.; Liu, G.; Liashenko, A.; Piskorz, P.; Komaromi, I.; Gomperts, R.; Martin, R. L.; Fox, D. J.; Keith, T.; Al-Laham, M. A.; Peng, C. Y.; Nanayakkara, A.; Gonzalez, C.; Challacombe, M.; Gill, P. M. W.; Johnson, B. G.; Chen, W. M.; Wong, W.; Andres, J. L.; Head-Gordon, M.; Replogle, E. S.; Pople, J. A. *Gaussian 03W, revision B.02*; Gaussian, Inc.: Pittsburgh, PA, 2003.
(42) Graf, D. L. *Am. Mineral.* **1961**, *46*, 1283–1316.
(43) Koretsky, C. M.; Sverjensky, D. A.; Sahai, N. *Am. J. Sci.* **1998**, *298* 349–438.
(44) Xiao, Y.; Lasaga, A. C. *Geochim. Cosmochim. Acta* **1994**, *58*(24), 5379–5400.
(45) Kubicki, J. D.; Bleam, W. F. *Molecular Modeling of Clays and Mineral Surfaces*; The Clay Mineral Society CMS Workshop Lectures, 2003; Vol. 12, p 229.

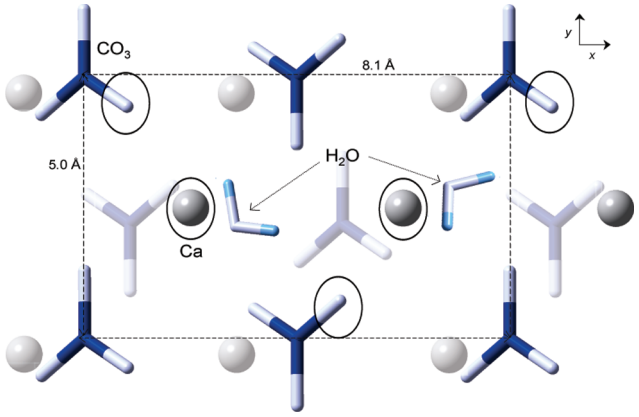

Figure 1. Plan view of the constituents of the $(CaCO_3)_9/2H_2O$ cluster. Ovals highlight "reactive" surface atoms that were allowed to relax in the optimizations in addition to H_2O monomers. Subsurface atoms are represented by shaded areas. Dashed line defines the surface unit cell. $x-y$ axes are arbitrary and agree with those selected in earlier studies.[18]

semi-ionic minerals such as $CaCO_3$, the use of standard point embedding techniques can be problematic because of possible polarization of cations near the borders of the cluster and because they cannot prevent unrealistic delocalization of the cluster wave function arising from the neglect of Pauli's exclusion effects.[46] Furthermore, the embedded point charges depend on the geometry and charge relaxation of the crystal surface, and therefore, the results must be subjected to validation against multiple point embedding models, a process that is both tedious and time-consuming.[38] Alternatively, stabilization of $CaCO_3$ surfaces can be improved by placing H_2O molecules in the vicinity of the exposed surfaces.[38]

Consequently, the use of sufficiently large charge-neutral cluster models, in combination with appropriate geometric constraints, is considered an adequate alternative to simulate semi-infinite calcium carbonate surfaces and minimize edge effects.[38,39] The selected cluster must realistically represent the mineral surface and the underlying bulk crystal to accurately describe local and long-range interactions while keeping the cluster size practical for ab initio calculations.[47]

In this study, the $Ca_n(CO_3)_n$ cluster size ranged from $4 \leq n \leq 18$ with a varying number of H_2O monomers, $0 \leq (H_2O)_n \leq 6$. The $Ca_9(CO_3)_9$ and $Ca_{18}(CO_3)_{18}$ clusters were used to represent one and two full surface unit cells, respectively. The surface atomic layer of the $Ca_9(CO_3)_9$ cluster was composed of 3 Ca atoms and 6 CO_3 groups, whereas the subatomic layer contained 3 CO_3 groups and 6 Ca atoms (Figure 1). In contrast, the composition of the surface and subsurface atomic layers of the $Ca_{18}(CO_3)_{18}$ cluster were identical: 9 $CaCO_3$ units in each layer (Figure 2). Most of our calculations were performed using these two clusters, which will hereafter be referred to, respectively, as the small and large cluster models. The selected density of H_2O molecules per surface area unit composing the first hydration layer (4.9 nm^{-2}) is consistent with the density of exchangeable surface Ca atoms (5 nm^{-2}), measured experimentally,[48] and reflects a 1:1 H_2O/Ca stoichiometry.

Preliminary all-atom RHF/6-31G(d,p) optimizations of small clusters, $Ca_4(CO_3)_4$ and $Ca_5(CO_3)_5$, were carried out for comparison with the geometry of the bulk crystal. These calculations revealed that, when all atom positions are allowed to relax, the cluster geometry is significantly distorted, particularly at the edges, and unrealistic interactions are obtained, such as several

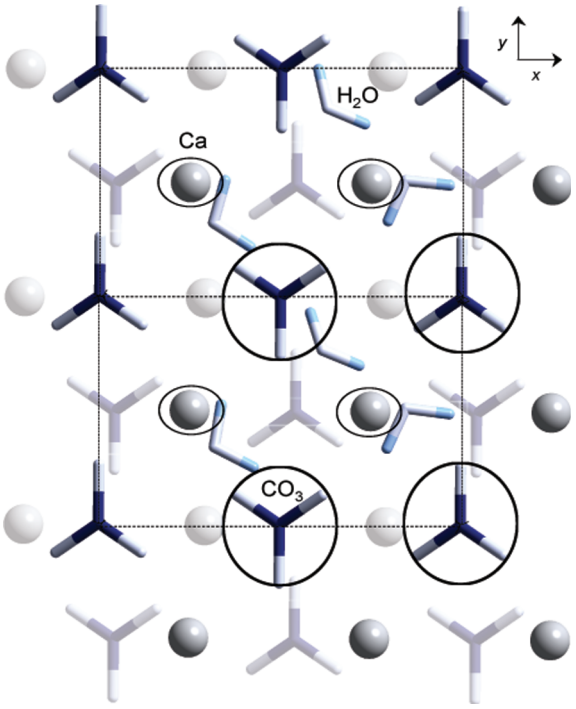

Figure 2. Plan view of the constituents of the $(CaCO_3)_{18}/6H_2O$ cluster. Ovals highlight "reactive" surface atoms that were allowed to relax in the optimizations in addition to H_2O monomers. Subsurface atoms are represented by shaded areas. Dashed lines define the two surface unit cells represented by the cluster model.

Ca atoms bonding directly to C atoms or to an unreasonable number of O atoms. Consequently, before performing further optimizations, criteria were developed to select the atoms whose positions could be restricted to those of the bulk structure. This step is critical to prevent the generation of unrealistic interactions between neighboring atoms and minimize computational time. To impose some control on the 3D symmetry of the selected cluster and mimic the bulk crystal, all the atoms present in the second atomic layer, the subsurface atoms, were fixed, and the computed geometry was examined for modifications in the coordination environment of both the surface and subsurface atoms. This condition was slightly modified later as explained below.

In adsorption studies, it is common practice to fully optimize the internal coordinates of the adsorbates while the surface atom positions are kept frozen.[39] However, this approach does not exploit the full potential of electronic relaxation offered by ab initio methods. It is more realistic to unlock some surface atoms, such as those that participate directly in the adsorption process, which will be referred to as "reactive" surface atoms throughout this paper. A careful selection of these geometric constraints will allow a more realistic description of the configuration of the hydrated surface layer and account for the interactions between the surface and the adsorbate (water) while controlling the 2D symmetry of the mineral surface and minimizing edge effects. The number of surface atoms allowed to relax must be selected on the basis of the adsorption reaction of interest, the cluster size, and the available computational capabilities.

Earlier theoretical studies[20,27−29,33,35] showed that each adsorbed H_2O, in the first hydration layer, interacts with one Ca and one or two O atoms at the (10.4) calcite surface. These "reactive" atoms are well-represented in our cluster models (Figures 1 and 2) and were allowed to relax during the cluster geometry optimizations. For the $Ca_9(CO_3)_9/2H_2O$ and $Ca_9(CO_3)_9/3H_2O$ clusters, all other surface atoms were frozen in their original crystallographic positions.

(46) Stefanovich, E. V.; Truong, T. N. *J. Chem. Phys.* **1997**, *106*, 7700–7705.
(47) Rosso, K. M. In *Molecular Modelling Theory: Application in the Geosciences*; Cygan, R. T., Kubicki, J. D. Eds.; Mineralogical Society of America, Rev. Mineral. Geochem.: Washington, DC, 2001; Vol. 42, p 199.
(48) Möller, P.; Sastri, C. S. *Zeit. Physik. Chem. Neue. Folg.* **1974**, *89*, 80–87.

To optimize computational time and prevent edge effects, water molecules were only allowed to interact with surface atoms within a full surface unit cell at the center of the large cluster surface. The initial position of the H_2O molecules in the first hydration layer were chosen to reflect results common to earlier studies: (i) herringbone adsorption pattern,[20,28] (ii) flat alignment of H_2O molecules[20,28,29] with respect to the surface, and (iii) H_2O oxygen atoms located at a distance of approximately 2.37 Å with respect to the surface calcium atoms.[20,29] On the basis of results of molecular dynamics[49] and X-ray scattering,[18] H_2O molecules in the second hydration layer, formally ascribed to the first hydration layer in earlier studies,[18,19,49] were initially placed at a greater distance from the surface (~3.3 Å), with a larger $x-y$ displacement from the surface Ca (~3.9 Å) and according to a 2:1 Ca/H_2O stoichiometry (Figure 2).

Results

Structural Details of the Hydrated Clusters. Preliminary cluster geometry optimizations of the small cluster models were performed using the STO3G and 3-21G basis sets for a quick comparison against the highest level of theory selected in this study, 6-31G(d,p). Very similar configurations of associatively adsorbed H_2O molecules were obtained with the 3-21G and the 6-31G(d,p) basis sets, with the interatomic distances between H_2O and the surface "reactive atoms" differing by less than 16%. In contrast, the STO-3G basis set predicted the dissociation of H_2O upon adsorption, whereas the position of H_2O constituents differed by up to 31% with respect to results generated by the 6-31G(d,p) basis set. Both the 3-21G and 6-31G(d,p) basis set simulations revealed that H_2O molecules do not lie flat on the mineral surface but are tilted with one of their H atoms pointing toward one of the "reactive" surface O atoms and the other pointing away from the surface. In other words, only one hydrogen bond can form between each H_2O monomer and the surface (see discussion below).

As in an earlier study,[29] to further confirm the associative adsorption character of H_2O, the adsorption of the H_2O constituents, H^+ and OH^-, on the calcite surface was simulated at the RFH/6-31G(d,p) level of theory using the small cluster. H^+ were initially bonded to surface O at 1 Å, and OH^- were bonded to surface Ca at the bulk crystal Ca−O bond length of 2.37 Å. The optimized structure revealed that the H^+ and OH^- spontaneously associated with H_2O with an identical configuration and SCF energy as when undissociated H_2O was considered as the initial configuration. That the 6-31G(d,p) basis sets predicts associative adsorption of H_2O from both initially dissociated and undissociated H_2O and yields identical $Ca_{(surface)}-O_{(water)}$ interatomic distances further supports its use in the optimization of larger $CaCO_3$ clusters.

The optimized interatomic distances of the Ca−O octahedra imply the substantial relaxation of the Ca−O bonds between the surface Ca and the subsurface O. The surface Ca atoms shift out from the surface, increasing their interatomic distances to subsurface O to the extent that the bond is substantially weakened (average $Ca_{(surface)}-O_{(subsurface)}$ bond length of 2.5 Å). To confirm this observation, we performed: (i) a geometric optimization of the $Ca_9(CO_3)_9/2H_2O$ cluster for which the subsurface O bonded to the surface Ca was unlocked and (ii) a geometric optimization of a three atomic layer cluster, $Ca_{12}(CO_3)_{12}$ + $2H_2O$, for which the entire CO_3 group in the second atomic layer associated with the surface Ca was unlocked (Figure 3) and the third layer was frozen to impose the bulk symmetry of the cluster. Both calculations confirmed the substantial relaxation of at least one Ca−O bond per surface Ca−O octahedron and yielded nearly identical structural results to those of the first RHF/6-31G(d,p) calculation.

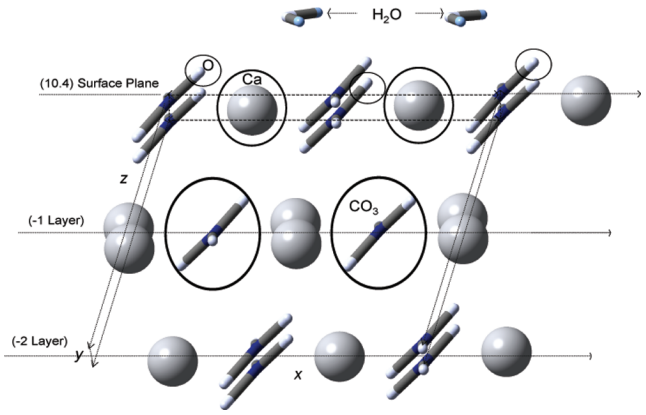

Figure 3. Snapshot of the $Ca_{12}(CO_3)_{12}/2H_2O$ cluster model. Ovals highlight reactive surface and subsurface atoms that were not frozen in the optimizations in addition to H_2O monomers. Two subatomic layers below the (10.4) surface are displayed. The approximate rhombohedral morphology of the cluster is defined by the dashed lines.

The optimized $Ca_{12}(CO_3)_{12}/2H_2O$ cluster shows that the Ca atoms move out of the surface, whereas the subsurface O atoms move away from the Ca both horizontally ($x-y$ directions) and vertically (z direction). As subsurface CO_3 groups relax, they rotate toward the subsurface plane (−1 layer in Figure 3) resulting in the stretching of more surface Ca−O bonds than in the small cluster without significantly affecting the average structure of the reconstructed surface. This observation validates the criteria we selected to impose geometric constraints and supports our premise that at least one Ca−O bond per surface Ca−O octahedron is significantly weakened, and approaches rupture, upon hydration. A thorough discussion on this issue is given below.

Having ascertained the self-consistency of our results using different cluster thicknesses, we can confidently focus on the results of the large clusters, $Ca_{18}(CO_3)_{18}/4H_2O$ and $Ca_{18}(CO_3)_{18}/6H_2O$, which provide a reasonable representation of the infinite calcite surface.

Although the calcite surface undergoes some reconstruction upon hydration, the average 2D dimensions of the (10.4) surface unit cell increase only by approximately 1% along the x direction, while they remain unchanged along the y direction (Figure 2). Table 1 summarizes the structural details of the reconstructed hydrated calcite surface for the $Ca_{18}(CO_3)_{18}/6H_2O$ cluster. They, respectively, reflect the average Cartesian and internal coordinates of the relaxed surface atoms and the H_2O. It is noteworthy that the Ca and C atoms are displaced differently along the three Cartesian coordinates. Their differential displacement along the z direction, normal to the surface, determines the height of the reconstructed surface layer, relative to the subsurface atomic layer, and yields the extent of surface relaxation. Conventionally, as in previous studies,[18] the averaged, relaxed positions of the Ca atoms were selected to define the reconstructed surface atomic layer and reference the position of H_2O in the hydration layer.

(49) Kerisit, S.; Parker, S. C. *Chem. Commun.* **2004**, *1*, 52–53.

Table 1. Average 3D Structural Registry of Calcium and Carbon Atoms at the (10.4) Calcite Surface and Internal Coordinates of Adsorbed Water Molecules in the First and Second Hydration Layer

3D displacement					surface atoms specification		
	surface atoms		H_2O monomers			surface	
Cartesian coordinates	calcium (Å)	carbon (Å)	1st hydration layer (Å)	2nd hydration layer (Å)	internal coordinates	relaxed	unrelaxed
X	0.05	0.43	0.56	2.06	carbon−oxygen (Å)	1.27	1.28
Y	−0.07	−0.22	0.08	2.26	calcium−oxygen (Å)	2.46	2.37
Z	0.17	−0.05	2.41	3.34	O−C−O angle (°)	120	120

Using the reconstructed lattice spacing, d_{12}, the average surface relaxation, δ_{12}, can be expressed as a percentage of the perfect lattice spacing, d, according to[50]

$$\delta_{12} = \frac{d_{12} - d}{d} \cdot 100 \quad (1)$$

An average surface relaxation of 5.6% relative to surface Ca was observed. The extent of surface corrugation is given by the surface rumpling parameter (Δ_z) which represents the difference between the z-coordinates of surface anions (Z^{anion}) and cations (Z^{cation}) with respect to the ideal lattice spacing:[50]

$$\Delta_z = \frac{z^{anion} - z^{cation}}{d} \cdot 100 \quad (2)$$

At the ideal (10.4) unreconstructed calcite surface, one O of each surface CO_3 lies 0.8 Å above the surface Ca and C atoms. Thus, the intrinsic rumpling (Δ_z) of the surface is 26.4% which, upon reconstruction, decreases to 24%. If the z-displacement of the central C of each CO_3, rather than the surface O, is considered relative to the surface Ca, the surface rumpling would go from zero for the unreconstructed surface, to 4.9% in the reconstructed surface. On reconstruction, the glide symmetry at the surface is slightly broken because of the differential displacement, along the z direction, of the surface Ca and the alternatively oriented CO_3 groups (Config-1 and Config-2 in Figure 4).

Upon hydration, surface Ca−O octahedra are distorted following changes in the Ca−O bond lengths. The average surface Ca−O bond length is stretched by ~4% (2.46 Å), 35% of the relaxed Ca−O bonds are stretched by less than 4.5% and one Ca−O bond per surface Ca−O octahedra stretches by at least 10%, whereas Ca−O bond contraction up to 5% is also observed in some Ca−O octahedra. Conversely, the CO_3 groups are not significantly distorted from their original trigonal planar geometry, although rigorously speaking, their D_{3h} symmetry is lost as a result of the differential displacement of the three O atoms along the z-axis (Figure 4). The average change in the CO_3 dihedral angle (O−C−O−O) is only 1.8°, which reflects the small out-of-plane distortion of the CO_3 group. The C−O bond lengths are only slightly shortened (<0.8%), whereas the average O−C−O angle remains unchanged. CO_3 groups are tilted toward the plane of the relaxed surface Ca atoms by an average of 4.1°, but their atomic positions along the $x-y$ directions are significantly modified (Table 1). Because of the relative rigidity of the CO_3 groups, their average $x-y$ displacement is expressed in terms of the optimized $x-y$ coordinates of the central C atom, the CO_3 center of mass, rather than relative to the surface O.

The associative character of adsorbed H_2O in the first and second hydration layers is confirmed in the large cluster, $Ca_{18}(CO_3)_{18}/6H_2O$. H_2O molecules in the first hydration layer (Mode-I) are slightly oblique to the surface with one H oriented toward one surface O and the other toward H_2O in the second hydration layer. H_2O molecules in the second hydration layer align their dipole nearly parallel to the surface (Mode-II). The average O−H−O angle of H_2O in the second hydration layer is smaller than that of H_2O in the first hydration layer, whereas the average O−H bond length of H_2O in both layers is identical, 0.95 Å. Nevertheless, H_2O in the second hydration layer displays a short (0.94 Å) and a long OH bond (0.97 Å), the longer being oriented toward surface O following hydrogen bonding (see below) and the shorter one pointing away from the surface. Structural details of the reconstructed calcite surface, including the two hydration layers modeled in this study, are illustrated in Figure 5.

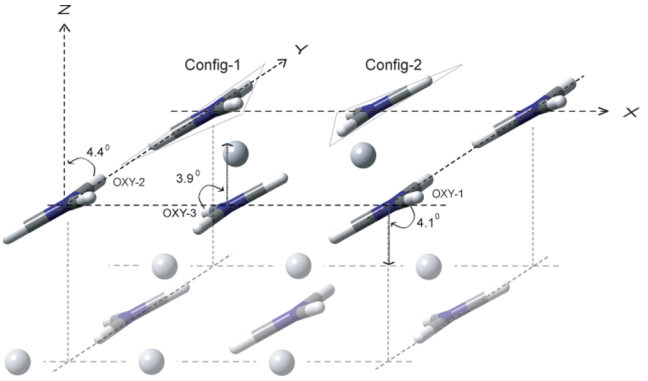

Figure 4. Schematic of the optimized (10.4) calcite surface displaying the average rotation of each oxygen atom in the carbonate groups along the z-axis. The two configurations adopted by the CO_3 groups within the surface unit cell are shown. Oxygens 1, 2, and 3 are, respectively, atoms protruding from the surface plane, aligned with the surface plane or below the surface plane. The trigonal planar geometry of the CO_3 group is not significantly perturbed. The average displacement of CO_3 groups along the $x-y$ direction is expressed in terms of the central carbon atom (see Table 1). Subsurface atoms are represented by shaded areas.

Energies of Adsorption. The energy of interaction between H_2O molecules and the calcite surface, E_{ads}, can be computed from[51]

$$E_{ads} = E_{slab/water}{}^{n} - (E_{slab} + n \cdot E_{water}) \quad (3)$$

where $E_{slab/water}{}^{n}$ represents the energy of the optimized cluster covered with $n H_2O$ molecules (n = 2, 4, or 6, depending on the cluster model) at their adsorption configurations, E_{slab} is the single-point energy of the cluster model with no H_2O attached (dry cluster model) and E_{water} is the energy of a single H_2O in the gas phase. The adsorption energy of $n H_2O$ attached to the cluster is equal to −172.8 and −306 kJ mol^{-1} for the small (n = 2) and large (n = 4) clusters, respectively. Upon

(50) Markmann, A.; Gavartin, J. L.; Shluger, A. L. *Phys. Chem. Chem. Phys.* **2006**, *8*, 4359.

(51) Cao, Y.; Chen, Z.-X. *Surf. Sci.* **2006**, *600*(19), 4572–4583.

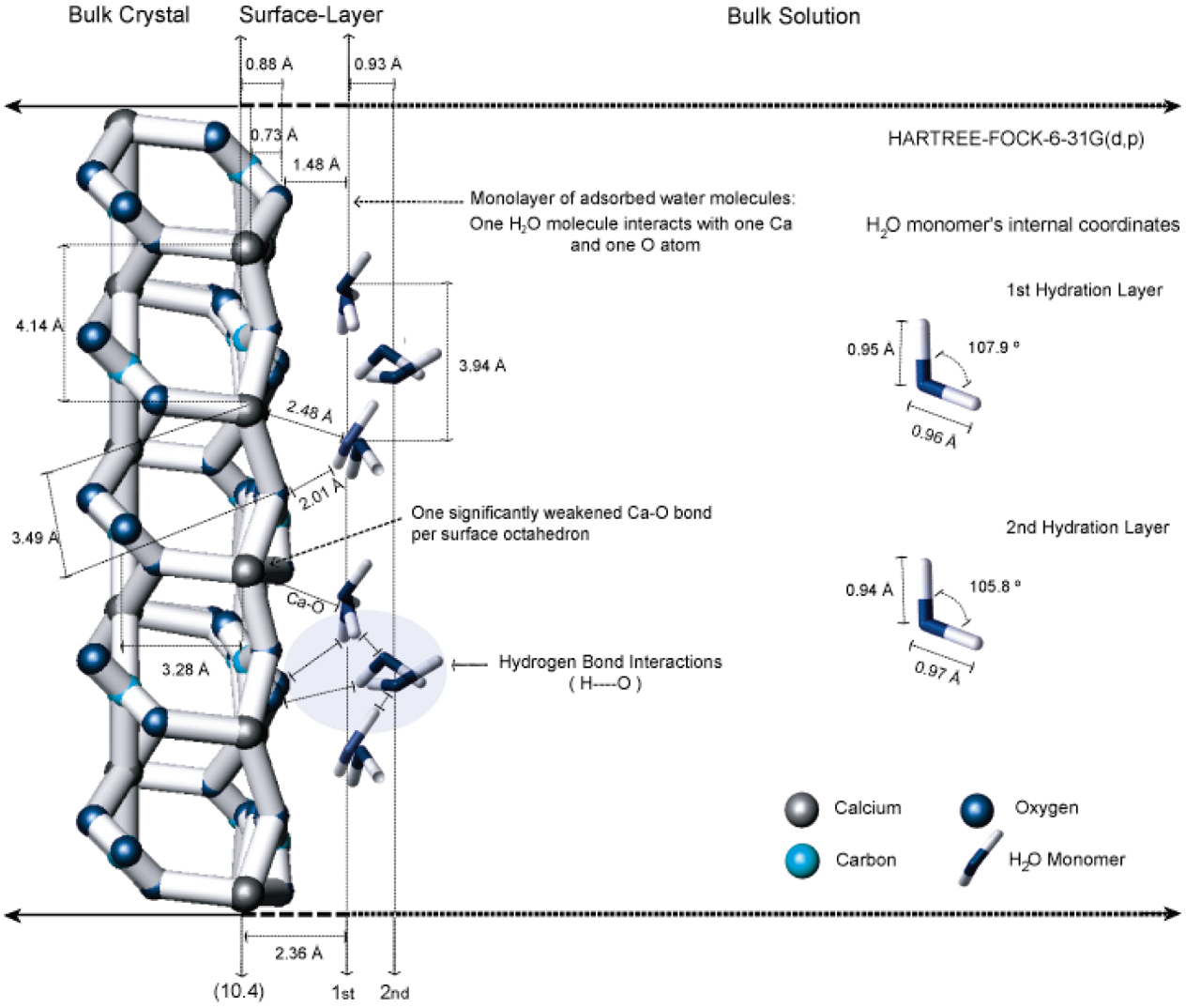

Figure 5. Lateral view of the (10.4) reconstructed calcite surface as predicted at the HF-6-31G(d.p) level of theory. Structural details of the first and second hydration layers are given. The average internal coordinates of the adsorbed water monomers are specified. Ca−O and hydrogen bond interactions are shown.

normalization to the number of attached H_2O monomers, their respective energies become −86.4 and −76.5 kJ mol^{-1}, corresponding to the binding energy of a single H_2O monomer at the cluster surface. The adsorption energy of the second hydration layer, $E_{ads\text{-}2nd}$, to the hydrated surface is given by

$$E_{ads-2nd} = E_{slab/water}{}^{6} - (E_{slab/1st} + 2 \cdot E_{water}) \quad (4)$$

where $E_{slab/1st}$ is the total energy of the large cluster with the four first layer H_2O monomers attached. Once normalized to the total number of adsorbed H_2O, $E_{ads\text{-}second}$ is −106.1 kJ mol^{-1}. To calculate the interaction energy between H_2O and the dry surface with no other adsorbates attached, the adsorption energy must be corrected by the average interaction energy, E_{inter}, among H_2O in the first and second hydration layers:[51]

$$E_{inter} = E_{water/1st/2nd} - (6 \cdot E_{H2O}) \quad (5)$$

where $E_{water/1st/2nd}$ is the single-point energy of the H_2O of the first and second hydration layers of the large hydrated cluster at their adsorbed configurations. To estimate E_{inter} for H_2O molecules constituting the first hydration layer, we subtracted the gas-phase single-point energy of four H_2O molecules from the single-point energy of the four H_2O molecules in the first hydration layer at their adsorbed configurations. In both cases, the estimated E_{inter} values per H_2O molecule are nearly equal (−11.9 kJ mol^{-1} for $n = 6$ and −12 kJ mol^{-1} for $n = 4$) and are in excellent agreement with the E_{inter} estimated by DFT calculations (−12.5 kJ mol^{-1} after basis set superposition error, BSSE, correction).[35] The agreement between the two independent energy estimates strongly supports the suitability of RHF methods, in combination with cluster models, to investigate hydration reactions at $CaCO_3$ surfaces, making computationally expensive periodic boundary condition calculations unnecessary.

Finally, the following energy decomposition:

$$E_{layer/slab} = E_{ads-layer} - E_{inter} \quad (6)$$

provides the individual interaction energy of H_2O in the first and second hydration layers with the dry surface ($E_{layer/slab}$), where $E_{ads\text{-}layer}$ corresponds to the interaction energy of a single H_2O molecule of either the first ($E_{ads\text{-}first\text{-}layer}$) or second ($E_{ads\text{-}second\text{-}layer}$) hydration layer and E_{inter} corresponds to the estimated interaction energy at each hydration layer. Equation 6 yields energies of −64.5 kJ mol^{-1} and −94.2 kJ mol^{-1} per

adsorbed H_2O molecule for the first and second hydration layers, respectively.

H_2O Interlayer Penetration. The surface reconstruction and weakening of the surface atomic layer that result from the relaxation of Ca−O bonds upon hydration may allow H_2O to penetrate the subsurface layers as is the case in other minerals such as scheelite ($CaWO_4$).[52] To model this effect, two additional H_2O were placed in the interlayer of the RHF/6-31G(d,p) optimized $Ca_9(CO_3)_9/2H_2O$ cluster and a geometric optimization of the $Ca_9(CO_3)_9/4H_2O$ cluster, with identical geometric constraints (i.e., freezing of subsurface lattice atoms and unlocking of "reactive" surface atoms and H_2O molecules) to those used for the small cluster, was performed. This optimization revealed that one of the H_2O remains undissociated and lies at the center of the subsurface interlayer with its dipole aligned normal to the surface, whereas the second H_2O is repelled and migrates toward one end of the cluster, dissociates, and interacts with atoms at the cluster edge forming $Ca-OH_{(water)}$ and $O-H_{(water)}$ bonds (see Supporting Information). The interlayer H_2O significantly stretches one $Ca_{(surface)}-O_{(surface)}$ bond (3.06 Å) whereas the average Ca−O bond stretching is 6% (2.52 Å). In addition to the Ca−O octahedra distortion induced upon hydration of the surface, following $Ca_{(surface)}-O_{(subsurface)}$ bond stretching, the subsurface H_2O further weakens the topmost atomic layer. The energy of H_2O incorporation from the bulk gas phase to the subsurface interlayer, E_{inc}, is computed from:

$$E_{inc} = E_{tot} - {E_{ads}}^2 \quad (7)$$

where, ${E_{ads}}^2$ is the energy of adsorption of two H_2O to the surface calculated with eq 3, whereas E_{tot} is the total energy of H_2O adsorption and interlayer incorporation as given for the $Ca_9(CO_3)_9/4H_2O$ cluster model by:

$$E_{tot} = {E_{slab/water}}^4 - (E_{slab} + 4 \cdot E_{H2O}) \quad (8)$$

Equation 7 yields a value of E_{inc} equal to -4.8 kJ mol^{-1}. Because of the vastly different configurations that H_2O molecules adopt upon incorporation into the calcite lattice, this value was not normalized to the number of H_2O molecules, and hence, it reflects the energy of incorporation of two H_2O molecules.

Discussion

Reliability of RHF/6-31G(d,p) Results. Proper evaluation of the accuracy of our theoretical predictions must be ultimately made against reliable experimental data. The only available experimental data describing the 3D structure of the hydrated calcite surface was obtained via X-ray scattering and GIXRD techniques.[18,19] Nevertheless, the uniqueness of a structural model derived from these techniques largely depends on their ability to resolve discrete, model-independent, structural features and to correct for systematic errors in the raw data exceeding the expected statistical error, issues difficult to address in practice.[53] More specifically, bond lengths derived from these X-ray measurements might incur systematic errors and should be treated with caution.[53] This is illustrated well by the differences between the structural models constructed from X-ray scattering and GIXRD data (e.g., equilibrium positions of surface atoms, interatomic distances), which makes it difficult to adopt one data set as "benchmark" for evaluating the accuracy of our theoretical results.

Alternatively, the accuracy of our uncorrelated RHF calculations, uncorrected for BSSE and zero point vibrational energy (ZPVE) effects, can be estimated by comparing published data acquired at different levels of theory ranging from uncorrelated RHF methods to higher levels of theory, accounting for electron correlation, BSSE, and ZPVE effects. Numerous first- and second-row element-containing polyatomic models have been studied at different levels of theory including RHF, DFT, and Møller-Plesset perturbation methods (MP2).[54−59] These studies revealed that, for moderate basis sets coupled with suitable polarization functions, e.g., 6-31G(d,p), MP2 approaches do not offer any substantial improvement over the less demanding uncorrelated, BSSE- and ZPVE-uncorrected RHF methods for the calculation of zeroth-order (e.g., structure, association and stabilization energies)[55,57−59] or second-order (e.g., harmonic frequencies, entropies and enthalpies)[54,56,59] chemical properties. In fact, in some cases (e.g., thermochemical quantities),[56,59] uncorrelated RHF and correlated DFT methods performed better than MP2, suggesting an intrinsic compensation of electron correlation, BSSE, and ZPVE effects. On the basis of these considerations and considering the excellent agreement of our results with those obtained with BSSE-corrected correlated DFT techniques (see above), we estimated the uncertainty of our RHF/6-31G(d,p) calculations to be ∼5%, which we believe to be an excellent compromise between accuracy and computational cost for the investigation of surface reactions at the ab initio level.

3D Structural Registry. Our results show that the hydrated calcite surface undergoes significant reconstruction upon hydration, including: bond relaxation, differential displacement of surface atoms along the *x*-, *y*-, and *z*- directions, and rupture of Ca−O bonds. This partly contrasts, qualitatively and/or quantitatively, with the results of some previous theoretical[20,26−29] and experimental studies.[18,19]

Associative adsorption of H_2O is observed under various adsorption scenarios, consistent with earlier results of atomistic studies,[20,27−29] molecular dynamic simulations,[32,33,48] and DFT[29,35] calculations. These common findings challenge the traditional idea that water hydrolysis products are attached to individual surface atoms upon dissociative H_2O adsorption.[10,60] Within the context of adsorption and surface complexation theory, the present results have fundamental implications to the definition of reactive surface sites, including charge and mass assignment that reflect on the formulation of mass action laws and the calibration of surface reactions.[61]

The configuration of adsorbed H_2O computed in this study is not flat relative to the surface[20,28,29] nor does it display a herringbone pattern.[20,28] The H_2O dipole in the first hydration layer lies slightly oblique to the surface. To minimize electrostatic repulsion between neighboring H_2O molecules, one of the H of adsorbed H_2O in the first hydration layer is oriented toward an O of the adjacent H_2O (H_2O_{adj}) in the second hydration layer, whereas the other H is oriented toward a surface O. This configuration is intermediate between those predicted by

(52) de Leeuw, N. H.; Cooper, T. G. *Phys. Chem. Chem. Phys.* **2003**, *5*, 433–436.
(53) Fenter, P.; Sturchio, N. C. *Prog. Surf. Sci.* **2004**, *77*, 171–258.
(54) deFrees, D. J.; McLean, A. D. *J. Chem. Phys.* **1985**, *82*(1), 333–341.
(55) Saebø, S.; Tong, W.; Pulay, P. *J. Chem. Phys.* **1993**, *98*(3), 2170–2175.
(56) Scott, A. P.; Radom, L. *J. Phys. Chem.* **1996**, *100*, 16502–16513.
(57) Maheshwary, S.; Patel, N.; Sathyamurthy, N.; Kulkarni, A. D.; Gadre, S. R. *J. Phys. Chem. A* **2001**, *105*(46), 10525–10537.
(58) Zhou, Z.; Shi, Y.; Zhou, X. *J. Phys. Chem. A* **2004**, *108*(5), 813–822.
(59) Rozmanov, D. A.; Sizova, O. S.; Burkov, K. A. *J. Mol. Struct. (Theochem)* **2004**, *712*, 123–130.
(60) Van Cappellen, P.; Charlet, L.; Stumm, W.; Wersin, P. *Geochim. Cosmochim. Acta* **1993**, *57*, 3505–3518.
(61) Villegas-Jiménez, A.; Mucci, A.; Pokrovsky, O. S.; Schott, J. *Geochim. Cosmochim. Acta*, in press.

atomistic and molecular dynamics studies: (i) flat orientation,[20,28,29] (ii) aligned near the surface with both H pointing to the surface,[27,33,34] and (iii) slightly angled above the surface with the two H pointing away from the surface.[26] The discrepancy reflects the chemical information contained in the RHF/6-31G(d,p) technique, which contrasts with the nonchemically informative force field-based calculations mentioned above. As expected, based upon the superior performance of electronic structure methods for the modeling of structural and energetic properties of minerals,[28] the RHF/6-31G(d,p) simulations agree best with results of the BSSE-corrected DFT calculations,[35] which also showed one H_2O hydrogen pointing to one surface O and the other H away from the surface.

The predicted average distance between surface Ca and $O_{(water)}$ atoms in the first hydration layer (2.48 Å) is in excellent agreement with values of earlier studies: atomistic simulations (2.35 to 2.73 Å)[20,25,27,30] and density functional theory (2.37 to 2.42 Å),[28,29,35] but contrasts with X-ray specular and nonspecular scattering[18] and grazing incidence X-ray diffraction (GIXRD) data[19] that yield interatomic distances of 2.97 Å and 2.1 Å, respectively. In the former case, the large $Ca-O_{(water)}$ distance was explained by a significant lateral displacement of H_2O relative to surface Ca along the *x*- and *y*-directions, whereas in the latter, no explanation was provided to explain such a short $Ca-O_{(water)}$ distance.

Estimated distances between the H atoms of H_2O in the first hydration layer and surface O atoms differ from earlier theoretical investigations. Results of the RHF/6-31G(d,p) simulations show that one of the water H points toward a surface O at a distance of 2.01 Å, suggesting hydrogen bonding, whereas the other H points away from the surface at an average distance of 3.3 Å from the nearest surface O, precluding hydrogen bonding with the surface (see next section). These results agree with DFT results (based upon the generalized gradient approximation, GGA)[28,29] inasmuch as the formation of one hydrogen bond per adsorbed H_2O ($H_{(water)}-O_{(surface)}$ distance of ~2.42 Å), but they differ with respect to the other $H_{(water)}-O_{(surface)}$ interatomic distance (~1.66 Å), which was assumed to reflect a second H-bond in that study. A much better agreement is obtained with BSSE-corrected DFT calculations that predict the formation of only one hydrogen bond and only slightly different $H_{(water)}-O_{(surface)}$ distances (1.81 Å and ~3 Å).[35] These discrepancies must reflect the absence of self interaction corrections in DFT[62] and improper treatment by the DFT functionals of the van der Waals (dispersion) attractive forces, arising from the long-range correlations of electronic density fluctuations,[63−65] which makes this technique less accurate than RHF/6-31G(d,p) in predicting hydrogen bonding and bridging. Furthermore, whereas DFT-GGA yields varying C−O bond lengths in CO_3 (1.29 to 1.37 Å),[28] the RHF/6-31G(d,p) optimized C−O bond lengths agree with the bulk calcite bond lengths to within 1%. The lack of explicit chemical information in atomistic calculations can explain why they predict the formation of two hydrogen bonds rather than the single one found in the present study and in an earlier DFT investigation.[35] Unfortunately, because of the weak X-ray scattering power of the H atoms, the structural models produced from least-squares fitting of X-ray scattering or GIXRD data are not sensitive enough to reliably determine the orientation of adsorbed water (no rotational degrees of freedom),[19] and therefore, comparisons of the internal coordinates of H_2O and H atoms positions against our results are unwarranted.

According to our RHF calculations, the H_2O molecules in the first hydration layer lie 2.36 Å from the surface, along the *z*-plane, in agreement with results of molecular dynamics (2.2 Å[31] and 2.3 Å[33]) and X-ray scattering (2.3 Å) studies.[18] The H_2O molecules in the second hydration layer sit 0.93 Å above the first hydration layer and 3.3 Å from the calcite surface, also in good agreement with molecular dynamics (3.2 Å[31] and 3.0 Å[33]) and X-ray scattering (3.45 Å) results.[18]

Upon hydration and relaxation of the calcite surface, atomistic simulations[27] and X-ray scattering[18] studies yield negative displacements of the Ca and C along the *z* direction. In contrast, results of this study predict a positive outward displacement of 0.17 Å, in good agreement with a recent molecular dynamics study (0.12 Å).[33] Our simulations revealed an $x-y$ displacement of H_2O molecules with respect to surface Ca atoms of 0.57 Å, much smaller than the one derived from X-ray scattering (1.9 Å)[18] but is in excellent agreement with results of molecular dynamics studies (0.6 Å),[31,66] which also consider the presence of multiple hydration layers near the surface to better represent solvent effects. It is noteworthy that these additional H_2O (or solvent) layers have been shown to have little effect on the bonded H_2O.[67] This further justifies our application of RHF techniques on sufficiently large $Ca_n(CO_3)_n$ clusters ($n \geq 18$) with a reduced number of H_2O (≥ 6) to adequately model the semi-infinite hydrated calcite surface, as usually represented in periodic DFT studies.

Disruption of the glide symmetry observed in our study (by 0.11 Å) arises from the differential displacement of Ca surface atoms along the *z* direction and contrasts with X-ray reflectivity[18] and GIXRD[19] data that show no evidence of such reconstruction and assume that the glide symmetry of the calcite surface is passed on to the hydration layer.[19] The observed loss of symmetry in our study is, however, compatible with results of atomic force microscopy (AFM) studies[12,13] that imply a vertical relaxation of approximately 0.35 Å[12] of the two alternatively oriented CO_3 groups within the surface unit cell (Figure 4) and agrees well with atomistic simulations of partially hydrated surfaces[20] that predict a differential displacement of the two CO_3 groups by 0.05 Å along the *z*-axis. Because AFM is believed to be plagued by technical artifacts (surface deformation by interaction with the probe tip), which may significantly overestimate the vertical relaxation of surface atoms,[12] a more subtle loss of symmetry, such as that suggested by the present results, is thought to be more realistic. Interestingly, in a more recent atomistic study,[68] a (2×1) reconstruction of the calcite surface (with rotation of half of the surface CO_3 groups) was predicted, and it was concluded that the extent of reconstruction largely depends on the experimental conditions which, in turn, may explain why surface reconstruction went undetected in some of the above-mentioned studies.

Bonding Relationships: Geometric and Energetic Criteria. On thermodynamic grounds, the formation of the first and second hydration layers is favorable, in agreement with earlier theoretical[20,27,28] and experimental findings[13] that indicate an

(62) Suba, S.; Whitehead, M. A. In *Recent Advances in Computational Chemistry- Vol. 1, Recent Advances in Density Functional Methods Part 1*; Chong, D. P., Ed.; World Scientific: New Jersey, 1995; pp 53−78.
(63) Ireta, J.; Neugebauer, J.; Scheffler, M. *J. Phys. Chem. A* **2004**, *108* 5692–5698.
(64) Santra, B.; Michaelides, A.; Fuchs, M.; Tkatchenko, A.; Filippi, C.; Scheffler, M *J. Phys. Chem.* **2007**, *127*, 184104.
(65) Santra, B.; Michaelides, A.; Fuchs, M.; Tkatchenko, A.; Filippi, C.; Scheffler, M *J. Phys. Chem.* **2008**, *129*, 194111.
(66) Parker, private communication in ref 18.
(67) Whitehead, M. A.; van de Ven, T. G. M.; Malardier-Jugroot, C. *J. Mol. Struct. (Theochem)* **2004**, *679*, 171–177.
(68) Rohl, A. L.; Wright, K.; Gale, J. D. *Am. Mineral.* **2003**, *88*, 921–925.

increasing stabilization of the (10.4) calcite surface following the adsorption of H_2O layers. At identical H_2O adsorption densities (two H_2O molecules per unit cell in the first hydration layer), the estimated adsorption or hydration energy per H_2O molecule in the first hydration layer, corrected for H_2O-H_2O interactions (-64.5 kJ mol^{-1}), lies within the range of values reported in earlier atomistic studies,[21,22,27,29] -53.9 to -93.9 kJ mol^{-1}, and is in excellent agreement ($\sim$3%) with the one estimated by BSSE-corrected DFT calculations also corrected for H_2O-H_2O interactions (-62.7 kJ mol^{-1}).[35] This suggests that the BSSE associated to our RHF/6-31G(d,p) calculations is either very small or is largely canceled out by other effects (e.g., correlation effects, ZPVE) not accounted for in our calculations (note that our E_{inter} differs by less than $\sim$5% from the BSSE-corrected DFT value;[35] see above). Unfortunately, the energy of adsorption of H_2O in the second hydration layer predicted in our study (-94.2 kJ mol^{-1}, corrected for H_2O-H_2O interactions) cannot be evaluated against experimental or other theoretical approaches, since this information is not available in any previous study.

The relaxation of surface atoms following hydration results in a significant weakening of some Ca−O bonds and of the topmost atomic layer of the calcite mineral with respect to the bulk. Because of steric hindrance, H_2O can only approach the mineral surface to within approximately 2.37 Å, the ideal Ca−O bond length in the bulk crystal structure. In response to their affinity for H_2O, Ca surface atoms are vertically displaced, increasing the interatomic distances of Ca to adjacent surface or subsurface CO_3 groups and relaxing and possibly breaking some Ca−O bonds. This can be analyzed in terms of bond valence theory,[69] an empirical approach based upon Pauling's valence sum principle[70] and parametrized on the basis of bulk crystal interatomic distances. Although the applicability of bond valence concepts to surface structures subjected to external stresses is controversial,[71] the progressive convergence of this theory with molecular-orbital models of chemical bonding[72] makes it a very promising approach to rationalize bond orders at reconstructed surfaces in terms of interatomic distances.

Using the RHF/6-31G(d,p) optimized Ca−O interatomic distances, we computed their respective bond valences from:[69]

$$S_{ij} = \exp\left(\frac{r_o - r_{ij}}{B}\right) \quad (9)$$

where S_{ij} is the bond strength for a given cation−anion pair (i, j) in valence units, v.u., r_0 is an empirical parameter specific to that pair of atoms (r_0 = 1.967 Å for Ca−O), r_{ij} represents the experimental bond length, and B is a fitted parameter equal to 0.37.[69] For all bonds formed by a given central atom, the valence sum principle must be satisfied:[69,70]

$$v_i = \sum_j S_{ij} \quad (10)$$

where v_i is the formal valence of the central atom i and the right-hand term is the calculated bond valence, v^{Calc}. Any deviations from v_i are typically considered to represent the unsatisfied or residual valence exhibited by atom i.[71] Nevertheless, it has been recently proposed that electronic and steric effects may generate substantial deviations from integer stoichiometric valences, v^{Stoich}, for some atoms and specific crystal structures.[73] This might be the case of bulk lattice Ca atoms, which are shown to exhibit a net increase in charge of $\sim$0.24 electrons per atom, slightly decreasing the divalent stoichiometric valence (v^{Stoich} = 2) typically ascribed to the Ca cation in calcite which, in turn, should give a structural valence (v^{Struct}) of 1.76.[74] Application of eqs 9 and 10 using the average optimized RHF/6-31G(d,p) Ca−O bond lengths (Table 2) yielded a v^{Calc} of 1.62 for the surface Ca atoms, significantly smaller than v^{Stoich}. In other words, in terms of bond valence and v^{Stoich}, it would seem that contraction of some Ca−O bonds do not fully compensate for the stretching of others, and hence, a net positive unsatisfied valence of approximately 0.4 v.u. per surface Ca atom is predicted. However, this unsatisfied valence would reduce to 0.14 v.u. if the structural valence predicted for Ca atoms in the bulk calcite lattice (v^{Struct} = 1.76)[74] applies to the surface as well. Alternatively, a hypothetical error of $\sim$4% in the r_0 value (for Ca−O interactions) would suffice to fulfill the valence sum principle, $v^{Calc} \cong v^{Stoich}$. Such an error would be compatible with the accuracy of the bond valence method for ionic compounds (5−7%)[75] and would fall within the variability of r_0 values designated for H−O ($\leq$25%),[76] O···H ($\leq$15%)[76] and lanthanide−O interactions (1−4%),[77] which show a dependency on the type or coordination number of the specific compounds used in r_0 calibration.

Regardless of the accuracy of the computed v^{Calc} values, the estimated S_{ij} values undoubtedly represent useful estimates of bond strengths which can be used as bond order indexes. Hence, as a rule, Ca−O bond valences reduced to $\leq$50% ($\sim$0.17 v.u.) of their bulk calcite value were considered to reflect very weak Ca−O bonds approaching rupture, which are hereafter referred to as "significantly weakened bonds" (SWBs). This reduction in bond valence corresponds to a cutoff bond length of $\geq$2.6 Å, which is equivalent to approximately 10% of bond stretching. Application of Emri's equation of bond orders[78] shows that the selected cutoff bond length corresponds to a bond order of 0.5, which is half of that in the bulk calcite lattice. This supports our premise that at distances of $\geq$2.6 Å, the Ca−O bond strength weakens to at least 50% of its value in the bulk crystal and substantiates our hypothesis that some Ca−O bonds may break upon hydration. Future extended X-ray absorption fine structure (EXAFS) investigations designed to resolve the coordination number, CN, of surface Ca atoms at hydrated cleavage calcite surfaces

Table 2. Average Relaxed Ca−O Bond Lengths Per Hydrated Surface Ca−O Octahedron[a]

bond ID	GIXRD[19]	this study
$Ca-O_{(1)}$	2.1	2.32
$Ca-O_{(2)}$	2.2	2.36
$Ca-O_{(3)}$	2.55	2.46
$Ca-O_{(4)}$	2.6	2.53
$Ca-O_{(5)}$	3	2.63

[a] Because Ca−O bond interactions are not explicitly identified by earlier authors,[19] Ca−O bond lengths of both studies are tabulated in ascending order. Sub-indexes are arbitrary identification labels.

(69) Brown, I. D. In *Structure and Bonding in Crystals*.; Vol. *2*, O'Keeffe, M., Navrotsky, A. Eds.; Academic Press: New York, 1981; pp 1−30.
(70) Pauling, L. *J. Am. Chem. Soc.* **1929**, *51*, 1010–1026.
(71) Bickmore, B. R.; Tadanier, C. J.; Rosso, K. M.; Monn, W. D.; Egget, D. L. *Geochim. Cosmochim. Acta* **2004**, *68*(9), 2025–2042.
(72) Burdett, J. K.; Hawthorne, F. C *Am. Mineral.* **1993**, *78*, 884–892.
(73) Wang, X.; Liebau, F. *Acta Cryst. Struct. Sci.* **2009**, *B65*, 96–98.
(74) Skinner, A. J.; LaFemina, J. P.; Jansen, H. J. F. *Am. Mineral.* **1994**, *79* 205–214.
(75) Brown, I. D.; Shannon, R. D. *Acta Crystallogr.* **1973**, *A29*(3), 266–282.
(76) Yu, D.; Xue, D.; Ratajczak, H. *J. Mol. Struct.* **2006**, *792−793*, 280–285.
(77) Zocchi, F. *J. Mol. Struct.(Theochem)* **2007**, *805*, 73–78.
(78) Emri, J. *J. Mol. Struct. (Theochem)* **2003**, *620*, 283–290.

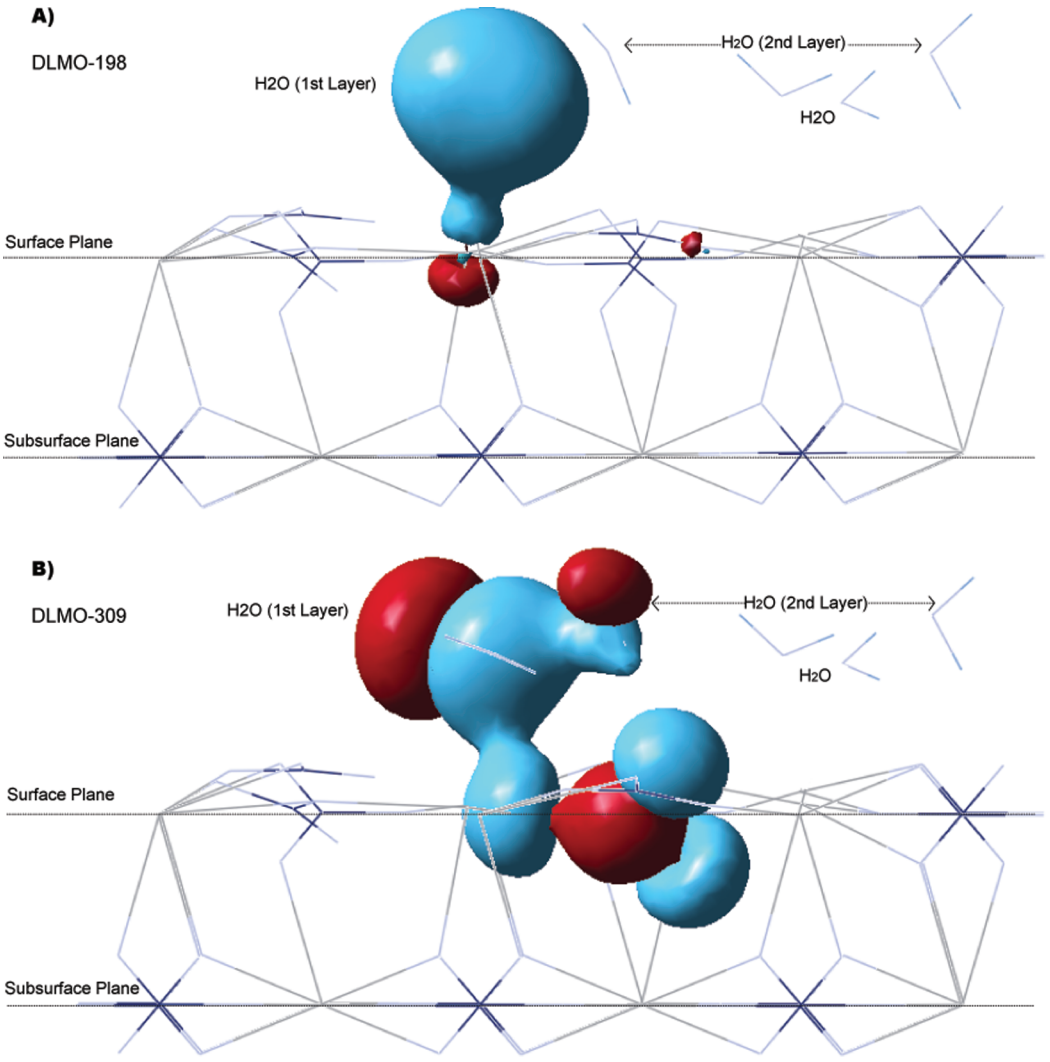

Figure 6. Delocalized molecular orbital (DLMOs) obtained from our large cluster RHF calculations displaying the chemical interactions between surface constituents and water molecules: (A) DLMO-198, $E = -1.41$ eV; $Ca_{(surface)}-H_2O$(1st hydration shell), and (B) DLMO-309, $E = -0.732$ eV, $Ca_{(surface)}-O_{(surface)}-H_2O_{(first\ hydration\ shell)}-H_2O_{(second\ hydration\ shell)}$.

will be instrumental in ascertaining whether the SWBs are part of the coordination shell of the central Ca atoms.

In Table 2, we show the average individual Ca−O bond lengths predicted in this study for wet conditions (six H_2O) as well as those obtained by an earlier GIXRD investigation.[19] It is noteworthy that, although the distortion of the Ca−O octahedron is observed in the dry and wet scenarios, the Ca−O stretching is more subtle in the former. For both scenarios, the ranges of Ca−O interatomic distances postulated by GIXRD data are broader (dry, 1.9−2.5 Å; wet, 2.1−3 Å) than in our study (dry, 2.3−2.4 Å; wet, 2.32−2.63 Å). Our predicted Ca−O bond lengths agree better with those estimated by an earlier atomistic study (dry, 2.3−2.7 Å; wet, unspecified bond lengths).[27] It follows that the disruption of the bulk crystal periodicity at the calcite surface leads per se to a detectable distortion of Ca−O octahedra, which increases upon interaction of the water layer with the calcite surface. Although earlier X-ray scattering data[18] also suggested a distortion of the surface Ca−O octahedra upon contraction of the in-plane Ca−O bond lengths and expansion of the $Ca_{(surface)}-O_{(water)}$ bond length, the Ca−O bond lengths are not specified in the study and comparisons are not possible.

The above considerations show that, in addition to the stabilizing effect of H_2O on the calcite surface, H_2O also plays an important role in the reorganization of Ca−O bonds. The significant relaxation of at least one Ca−O bond per surface Ca atom reflects the strong affinity of Ca for H_2O and must therefore be a precursory step to the eventual release of surface Ca atoms to the bulk solution which, in turn, may lead to a provisional nonstoichiometric calcite dissolution regime. It is worth noting that earlier findings could also be taken as indirect evidence of the preferential dissolution of Ca atoms over CO_3^{2-} ions by H_2O following the stabilization of the hydrated mineral surface. For instance, DFT calculations[34] revealed that, at 100% relative humidity, a nonstoichiometric, calcium-deficient surface may predominate over the ideal (10.4) stoichiometric termination, whereas XPS data showed a slight depletion in both O and Ca relative to C atoms in the surface of dissolving calcite samples.[10] Furthermore, interpretations of the electrokinetic behavior of calcite in aqueous suspensions suggest the greater tendency of Ca^{2+} than CO_3^{2-} ions to pass into solution.[79] Finally, recent acid−base surface titrations of calcite suspensions revealed that Ca^{2+} is released in exchange for H^+ under

(79) Douglas, H. W.; Walker, R. A. *Trans. Faraday Soc.* **1950**, *46*, 559–568.

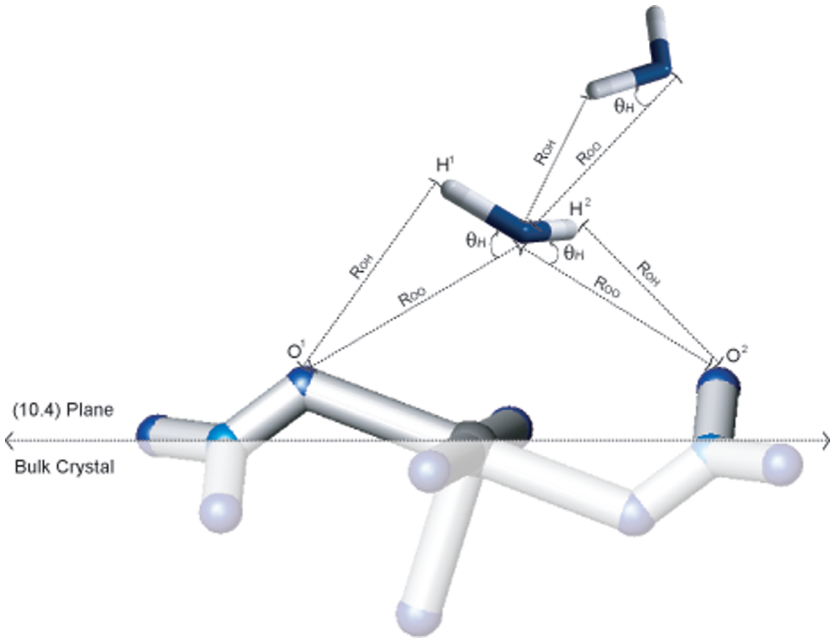

Figure 7. Geometric definition of the hydrogen bond[83−85] established between H_2O molecules and surface atoms and among adjacent H_2O molecules. The optimized orientations of H_2O molecules in the first and second layer are slightly modified for clarity.

circumneutral and alkaline conditions, reflecting the strong susceptibility of Ca atoms to leave the surface.[80]

It has also been hypothesized that Ca−O bonds may break upon attachment of protons to the calcite surface (via bonding to surface O atoms) under acidic conditions,[81] but the weakening or rupture of Ca−O bonds following the adsorption of H_2O has not been postulated before. Furthermore, our results show that H_2O in the first hydration layer may diffuse to the subsurface interlayer, further weakening the topmost layer by rupture of additional Ca−O bonds. We did not thoroughly examine the effect of H_2O interlayer incorporation on the stability of the calcite surface, but we believe that this mechanism deserves further investigation, as it possibly plays a key role on mineral dissolution, rearrangement of surface layers, ion replacement, and solute transport through subsurface lattice layers in aqueous solutions.

The similarity in the bond lengths between surface Ca and H_2O (2.48 Å) with Ca−O bonds in the bulk lattice (2.36 Å) and the strong interaction between a single H_2O and the calcite surface ($E_{ads\text{-}first\text{-}layer} = -64.5$ kJ mol^{-1}) suggests similarities between the character of binding of the $Ca_{(surface)}-O_{(water)}$ and the $Ca_{(surface)}-O_{(calcite)}$ bonds. Although the latter has been traditionally considered ionic, there is some theoretical evidence that the 3p orbital of Ca may hybridize slightly with the 2s and 2p orbitals of C and O and, therefore, contribute to the electron density on the C−O bond in CO_3, implying some covalent character.[35] In contrast, the bond valence scale only ascribes a covalent character to bonds with bond valences of ≥0.6,[82] which is not the case of the Ca−O interactions observed in our study. Regardless of whether the $Ca_{(surface)}-O_{(water)}$ interaction is purely ionic or not, our findings are consistent with experimental results confirming the chemisorption of H_2O molecules in direct contact with the calcite surface.[4]

H_2O−calcite surface interactions are illustrated by the delocalized molecular orbitals, DLMO-198 and DLMO-309, in Figure 6. DLMO-198 shows a local interaction between H_2O in the first hydration layer and a surface Ca, whereas in DLMO-309, the interaction involves Ca, C, and O surface atoms and H_2O molecules in the first and second hydration layers. They show that, in the first layer, H_2O is directly bonded to the surface Ca while interacting, through hydrogen bonding, with surface O and adjacent H_2O in the second hydration layer.

Table 3. Geometric Coordinates Confirming the Formation of Hydrogen Bonds between H_2O Molecules and Calcite Surface Atoms as Well as among Adjacent H_2O Molecules

	internal coordinates		
type of interaction	R_{OH} (Å)	R_{OO} (Å)	θ_H (°)
$H_2O_{(first\text{-}layer)}$−surface oxygen	2.01	2.82	26.4
$H_2O_{(second\text{-}layer)}$−surface oxygen	1.78	2.75	3.9
$H_2O_{(first\text{-}layer)}-H_2O_{(second\text{-}layer)}$	2.04	2.9	18

The formation of hydrogen bonds between water and surface atoms and between pairs of adjacent adsorbed water monomers can be discussed within the context of the geometry of the hydrogen bond, as previously done for liquid water[83] and a large number of aqueous mixtures.[84−86] Under this scheme, the hydrogen bond is defined by geometric criteria and maximum internal coordinates.[85] These coordinates are illustrated in Figure 7 for the calcite surface−H_2O and H_2O-H_2O interactions. Let R_O represent either the oxygen in the CO_3 group or in the H_2O molecule; then, R_{OO} represents the interatomic distance between the oxygen of the bridging H_2O molecule and R_O, θ_H is the angle between the H−O bond of H_2O and R_O, and R_{OH} is the length of the hydrogen bond.

The cutoff values are those specified earlier for H_2O-H_2O interactions:[86] $R_{OO} \leq 3.5$ Å, $R_{OH} \leq 2.45$ Å, and $\theta_H \leq 30°$. This geometric approach is convenient since it applies to discretely H-bonded molecules and can be generalized directly to systems other than water and water-like systems.[83]

(80) Villegas-Jiménez, A.; Mucci, A.; Paquette, J. *Phys. Chem. Chem. Phys.*, in press.
(81) Sjöberg, E. L. *Stockholm Contrib. Geol.* **1978**, *32*(1), 1–92.
(82) Altermatt, D.; Brown, I. D. *Acta Crystallogr.* **1985**, *B41*, 240–244.
(83) Mezei, M.; Beverdige, D. L. *J. Chem. Phys.* **1981**, *74*(1), 622–632.
(84) Ferrario, M.; Haughney, M.; McDonald, I. R.; Klein, M. *J. Chem. Phys.* **1990**, *93*(7), 5156–5166.
(85) Luzar, A.; Chandler, D. *J. Chem. Phys.* **1993**, *98*(10), 8160–8173.
(86) Chowdhuri, S.; Chandra, A. *Phys. Rev. E* **2002**, *66*, 041203−1–7.

On the basis of these criteria (Table 3), one hydrogen bond is formed between H_2O in the first hydration layer and a surface O (O^2-H^2 in Figure 7), and in agreement with atomistic studies,[20,27] there is no hydrogen bond between adjacent H_2O in the first hydration layer. In addition, H_2O of the second hydration layer are hydrogen-bonded to a surface O atom and to one adjacent H_2O in the first hydration layer (Figure 5).

In agreement with earlier findings,[20] the hydrogen bond network within the first hydration layer is disrupted by its strong interaction with the surface. Ordering of the second hydration layer cannot be properly evaluated with this model because only two H_2O monomers are used to model this layer and the influence exerted by adjacent multiple H_2O layers is neglected. However, as emphasized earlier, solvent effects are most likely negligible,[67] and therefore, the results are considered reliable first-order descriptors of the second hydration layer registry obtained, for the first time, at the ab initio level.

The different nature of the interaction established by H_2O in the second layer (hydrogen bonding) and by H_2O in the first layer (ionic and hydrogen bonding) with the surface is consistent with thermogravimetric[4,5] and Fourier-transformed infrared data[5] revealing the presence of strongly adsorbed H_2O, "chemisorbed", and weakly adsorbed H_2O, "physisorbed", at hydrated calcite surfaces.

Conclusions

The power of ab initio RHF molecular orbital methods, coupled to moderately large cluster models and adequate basis sets, was exploited to investigate the ground-state structural, energetic properties, and bonding relationships of the hydrated (10.4) calcite surface. Fresh insights into the 3D structural registry and adsorption energetics of the first and second hydration layers at the reconstructed (10.4) calcite surface complement the information derived from earlier atomistic and X-ray scattering and GIXRD studies.

Whereas small discrepancies in the configuration of adsorbed H_2O molecules and their lateral registry are observed with respect to results of atomistic and molecular dynamic studies, in general, there is good agreement with earlier DFT calculations, especially with those corrected to the BSSE. The extent of surface reconstruction upon hydration is more important than previously suggested. This includes bond stretching and the differential 3D displacement of surface atoms which results in surface relaxation (5.6%) and a decrease in the intrinsic surface rumpling (2.4%) following the rotation of CO_3 groups toward the surface.

The stabilizing effect of associatively adsorbed water on the (10.4) calcite surface, previously postulated by atomistic and DFT studies, was confirmed at the RHF/6-31G(d,p) level of theory. The formation of two ordered hydration layers is thermodynamically favorable where each H_2O in the first hydration layer is bonded to a single surface Ca by ionic bonding and to a surface O by a hydrogen bond. There is therefore "chemisorption" of H_2O to the calcite surface, as shown by experiment. According to geometric criteria, the strong H_2O−surface interaction disrupts the hydrogen bond network of H_2O in the bulk solution, which prevents hydrogen bonding between adjacent H_2O in the first layer. H_2O in the second layer hydrogen bonds with a surface O and with adjacent H_2O in the first layer, reflecting a weaker interaction with the surface relative to H_2O in the first layer. This interaction is interpreted as H_2O "physisorption", in agreement with earlier experimental data.

Most noteworthy is the role that H_2O plays in the reorganization of Ca−O bonds at the calcite surface. In agreement with X-ray scattering and GIXRD results, surface Ca−O octahedra undergo substantial distortion upon H_2O binding to Ca, but in constrast to earlier suggestions,the sixfold coordination shell of surface Ca atoms is probably not restored because of the relaxation of surface atoms. This significantly weakens at least one Ca−O bond per surface Ca atom and possibly leads to bond rupture. Alternate methods such as EXAFS techniques must be applied in future studies to determine the CN of surface Ca atoms and confidently ascertain whether the SWBs at the hydrated (10.4) calcite surface reflect bond breaking or not. We conclude that, to stabilize the hydrated surface, H_2O may provisionally dissolve surface Ca preferentially over CO_3 groups. This observation is critical in the understanding of molecular mechanisms of mineral dissolution, rearrangement of surface layers, ion replacement, charge development, and solute transport through subsurface lattice layers.

Acknowledgment. A.V.-J. thanks Prof. Theo G. M. van de Ven for critical discussions at earlier stages of this investigation as well as Dr. Nora de Leeuw, Dr. Kate Wright, and Dr. Paul Fenter for providing additional information on their results. The constructive comments provided by two anonymous reviewers have substantially improved the quality of our work. This research was supported by a student grant to A.V.-J. from the Geological Society of America (GSA) and by the Natural Sciences and Engineering Research Council of Canada (NSERC) through Discovery grants to M.A.W and A.M. A.V.-J. also received postgraduate scholarships from Consejo Nacional de Ciencia y Tecnología of Mexico and benefited from additional financial support from Consorcio Mexicano *Flotus-Nanuk*, the Department of Earth and Planetary Sciences of McGill University and the GEOTOP-McGill-UQAM Research Centre.

Supporting Information Available: The Cartesian coordinates of the optimized small and large cluster models (dry and hydrated) are available. A schematic illustration of the optimized calcite structure following the incorporation of H_2O into the subsurface interlayer and a comprehensive list of RHF runs performed in this study are also provided. This material is available free of charge via the Internet at http://pubs.acs.org.